

Nonalcoholic fatty liver disease is associated with an altered hepatocyte microRNA profile in LDL receptor knockout mice[☆]

Menno Hoekstra^{*}, Ronald J. van der Sluis, Johan Kuiper, Theo J.C. Van Berkel

Division of Biopharmaceutics, Leiden/Amsterdam Center for Drug Research, Gorlaeus Laboratories, P.O. Box 9502, 2300RA Leiden, The Netherlands

Received 17 August 2010; received in revised form 11 February 2011; accepted 4 March 2011

Abstract

MicroRNAs modulate processes associated with cell cycle control and differentiation. Here we explored the potential of microRNAs in the modulation of hepatic lipid metabolism and the development of nonalcoholic fatty liver disease.

MicroRNA profiles of hepatocytes from low-density lipoprotein (LDL) receptor knockout mice fed a chow diet or a hypertriglyceridemia/fatty liver-inducing Western-type diet (WTD) were determined using quantitative real-time polymerase chain reaction. Ninety-seven of 103 microRNAs measured were expressed by hepatocytes and low variability between hepatocyte pools was observed. Feeding WTD coincided with a marked fivefold decrease in the relative expression level of miR-216 ($P < .05$) and miR-302a ($P < .01$). Interestingly, an increased hepatic miR-216 expression was detected in response to fasting. MicroRNA/biological function linkage analysis suggested that the change in hepatocyte microRNA profiles in response to high dietary lipid levels is associated with changes in cell cycle control and proliferation. In accordance with a diminished miR-302a expression on the WTD, hepatocyte mRNA expression levels of miR-302a target genes *ABCA1* and in particular *ELOVL6* were increased in response to WTD (twofold to ninefold). This suggests a role for miR-302a in hepatic cholesterol, fatty acid and glucose metabolism.

In conclusion, we have shown that fatty liver development in LDL receptor knockout mice is associated with a significant change in the hepatocyte microRNA profile, i.e., a fivefold decrease in miR-216 and miR-302a expression. Based upon our comparative gene and microRNA expression studies it is anticipated that miR-302a may prove to be a valuable therapeutic target in the regulation of hepatic fatty acid utilization and insulin resistance.

© 2012 Elsevier Inc. All rights reserved.

Keywords: MicroRNA; Hepatocytes; Liver steatosis; Nonalcoholic fatty liver disease; Lipid metabolism; Fasting

1. Introduction

Nonalcoholic fatty liver disease (NAFLD) is characterized by the accumulation of lipid in liver cells (hepatic steatosis) and forms the most common cause of liver disease (reviewed by Jou *et al.* [1]). The intra-hepatic lipid balance is maintained by different processes including receptor-mediated uptake of lipids, *de novo* synthesis of lipids, secretion of lipids into the bile and the blood compartment and hepatic storage of lipids. Perturbations in the activity of essential mediators functioning in these processes can induce disturbances in the intrahepatic lipid homeostasis. More specifically, when the input of lipid exceeds the output of lipid from the liver, this will induce excessive storage of lipid and thus lead to the development of hepatic steatosis. Nonalcoholic fatty liver disease may slowly progress into nonalcoholic steatohepatitis (NASH), which is characterized by excessive liver inflammation. Nonalcoholic steatohepatitis is an

established risk factor for the development of end-stage liver disease (i.e., cirrhosis), a condition that generally can only be treated by performing a liver transplantation.

MicroRNAs constitute an important class of highly conserved noncoding RNAs that inhibit the protein expression of their target genes through modulation of the mRNA translation rate and/or stability [2]. Recent studies have indicated that the hepatic expression profile (signature) of microRNAs is significantly different in subjects with NASH vs. controls with normal liver histology [3]. Importantly, although microRNAs are primarily known for their role in cell cycle regulation and cell differentiation [4,5], microRNAs such as miR-122 have also been shown to modulate the expression of genes involved in lipid metabolism [6,7]. Alterations in the microRNA signature may thus underlie the metabolic changes that result in the initial formation of hepatic steatosis and subsequent development of NASH. Initial microRNA profiling studies in whole liver specimens in mice have already been executed to identify microRNA targets that may be crucially involved in hepatic lipid metabolism and steatosis development [8]. However, the liver is a complex tissue that consists of several different cell types that each play a distinct role in hepatic metabolism. We have previously shown that, for studies on the function/expression of genes, it is important to take their intrahepatic

[☆] This research was supported by Top Institute Pharma (TIPharma project T2-110; M.H. and T.V.B.) and by grant 2008T070 (M.H.) from the Netherlands Heart Foundation.

^{*} Corresponding author. Tel.: +31 71 5276238; fax: +31 71 5276032.
E-mail address: hoekstra@lacdr.leidenuniv.nl (M. Hoekstra).

cellular localization into account [9–11], and we anticipate that the same accounts for microRNAs. Hepatocytes, also known as liver parenchymal cells, represent the primary metabolic cell type within the liver and disturbances in the expression of key genes involved in hepatocyte lipid metabolism have been associated with the development of fatty liver and cholestasis both in animal models and man [12–14]. In the current study, we have investigated with a commercially available validated real-time polymerase chain reaction (PCR)-based platform the hepatocyte-specific microRNA signature of 103 murine microRNAs in an established hyperlipidemic mouse model of NASH—Western-type diet (WTD)-fed low-density lipoprotein (LDL) receptor knockout mice [15,16]—to identify microRNAs that can possibly be used as therapeutic targets to inhibit the development of hepatic steatosis and end-stage liver disease.

2. Materials and methods

2.1. Animals

Homozygous LDL receptor knockout (LDLR^{−/−}) mice were obtained from the Jackson Laboratory as mating pairs and bred at the Gorlaeus Laboratories, Leiden, The Netherlands. Mice were maintained on a regular chow diet containing 5.7% (w/w) fat and no cholesterol (RM3, gross energy content=15.11 MJ/kg; Special Diet Services, Whitham, UK) or were fed a semisynthetic WTD containing 15% (w/w) cocoa butter and 0.25% (w/w) cholesterol (Diet W, gross energy content=18.73 MJ/kg; Special Diet Services). Mice were fed *ad libitum* or fasted overnight (~16 h) and subsequently anesthetized, sacrificed. After whole body perfusion with PBS, livers were isolated and immediately frozen in liquid N₂ and stored at −80°C until RNA extraction. Animal experiments were performed at the Gorlaeus Laboratories of the Leiden/Amsterdam Center for Drug Research in accordance with national laws. All experimental protocols were approved by the Ethics Committee for Animal Experiments of Leiden University.

2.2. Oral glucose tolerance test

Mice were fasted for 16 h after food withdrawal at 5:00 p.m. At 9:00 a.m. the next day, mice were subjected to an oral glucose tolerance test (OGTT). This procedure began with a blood sample collection using a manual ACCU-CHEK Compact glucose monitor ($t=0$ min), immediately followed by an oral gavage of 2 g/kg D-glucose as a 25% solution in sterilized 0.9% NaCl. Additional blood samples were analyzed for blood glucose concentrations via tail bleeding at 15, 30, 45, 60, 90, 120 and 180 min after the oral glucose administration. Based upon the obtained glucose vs. time profiles, the glucose area-under-the-curve (AUC) for each mouse was calculated using GraphPad Prism software.

2.3. Hepatocyte isolation

Hepatocyte fractions that consist of pure hepatocytes as judged by light microscopy and which do not express the macrophage marker CD68 as determined by quantitative gene expression analysis were isolated as described [11]. Mice were anaesthetized and the vena cava inferior was cannulated. Subsequently, the vena porta was ligated and the liver was perfused for 10 min (14 ml/min) with oxygenated Hanks' buffer pH 7.4, containing HEPES (1.6 g/l). The perfusion was continued for 10 min with Hanks/HEPES buffer containing 0.05% (w/v) collagenase (Type IV, Sigma) and 1 mM CaCl₂. Hepatocytes were isolated after mincing the liver in Hanks' buffer containing 0.3% bovine serum albumin, filtering through nylon gauze and centrifugation thrice for 10 min at 50×g.

2.4. Quantitative microRNA expression analysis

Stem-loop quantitative real-time reverse transcriptase (RT)-PCR analysis for the detection of 103 different microRNAs was performed using the commercially available Applied Biosystems Taqman microRNA platform essentially as described [17]. Total RNA was isolated from hepatocytes using the established guanidium thiocyanate/phenol/chloroform RNA extraction method of Chomczynski and Sacchi [18]. Ten nanograms of RNA from two pooled RNA samples of two mice (total of four mice) was mixed with a reverse transcriptase (RT) master mix containing dNTPs, multiscribe RT enzyme, RT buffer, RNase inhibitor and microRNA-specific RT primers. The reverse transcription reaction was carried out in an AB7500 fast thermal cycler for 30 min at 16°C, 30 min at 42°C and 5 min at 85°C. The generated microRNA-specific cDNA was mixed with Taqman 2X Universal PCR master mix (NO AmpErase UNG) and microRNA-specific Taqman MicroRNA probes (20×) and subjected to fluorescent real-time quantitative PCR analysis using the AB7500 Fast System using the following PCR program: 95°C for 10 min and 40 cycles of 15 s at 95°C and 1 min at 60°C. For sequences of the miRNA-specific probes used, refer to Table 1. Within the microRNA, RT-PCR kit manufacturing and

Table 1

Probes used for quantitative real-time PCR-based miRNA profiling

miRNA target	Probe sequence	miRNA target	Probe sequence
let-7a	ugagguaguagguuauaaguu	miR-189	gugccuacugagcugauaagcu
let-7b	ugagguaguagguuguguguu	miR-190	ugauauuuuaguuauuuaggu
let-7d	agagguaguagguugcauagu	miR-191	caacggaaucuccaaaagcagcu
let-7e	ugagguagaggguuauaagu	miR-193	aacuggccuacaaaguccag
let-7g	ugagguaguaguuuuuacagu	miR-194	uguaacagcaacucacugugga
let-7i	ugagguaguaguuuugucu	miR-195	uagcagcacagaaauuuggc
miR-100	aaccguagauagcgaacuugug	miR-199a	cccaguguuacagacuaccguuuc
miR-103	agcagcauuuguacagggucauga	miR-199a*	uacagugucugcacaauugguu
miR-107	agcagcauuuguacagggucauca	miR-19a	ugugcaaaucuaugcaaaacuga
miR-10a	uaccguagauagcgaauuugug	miR-200a	uaacacugucugguuaacgaugu
miR-122a	uggagugugacaaugguuguuu	miR-200c	aaucacugccggguuaugaugga
miR-124a	uaaggcgacgcggguuagucca	miR-205	uccuucuuuuccacggagucug
miR-125a	uccucgagaccuuuaacugug	miR-21	uagcuuaucagacugauuguu
miR-125b	uccucgagaccuuuaacuguga	miR-210	cugugcugugagcagcgguug
miR-126	ucguacggugagaauaauugc	miR-213	accuacgacccuugauuugacc
miR-127	ucggauccgucugagcuuggc	miR-214	acagcaggcacagacaggcag
miR-128a	ucacagugaacggucucuuuu	miR-216	uaucucagcugggcaacugug
miR-128b	ucacagugaacggucucuuuuc	miR-218	uugugcuuagcuuaaccaugu
miR-130a	cagugcauuguuuaaaggcg	miR-219	ugauuuguccaaacgcaauuc
miR-130b	cagugcauuguuuaaaggcg	miR-222	agcuacacugcugcucugugcu
miR-132	uaacagucucagcgaugucug	miR-223	ugucaguuuugcaaaucuccc
miR-133a	uaggucuccuuaacacgcuu	miR-23a	aucacauugccagggaauuucc
miR-133b	uaggucuccuuaacacgcuu	miR-23b	aucacauugccagggaauuucc
miR-134	ugugacugguuagcagagggg	miR-25	cauugcacuugucugggucuga
miR-135a	uauggcuuuuuuauuccuaguga	miR-26a	uucaaguuuacaggauagggcu
miR-135b	uauggcuuuuuuauuccuaguga	miR-27b	uucacagugggcuagguucug
miR-137	uaugcuuaaagaauacgcguag	miR-28	aaggagcucacagucuaauagag
miR-138	agcugugugugugauuac	miR-296	aggggccccccuuaacucguu
miR-139	ucuaacagugcagcugucu	miR-299	ugguuuuacggucccauacau
miR-140	agugguuuuacccuauugguag	miR-29a	cuagcaccuacugaaauccguu
miR-141	aacacugucugguuaaagauug	miR-29c	uagcaccuuuugaaucggguu
miR-142-5p	cauaaagugagaagacacuac	miR-301	cagugcaauaguuuugcaaaagc
miR-144	uacaguuuagauaguuacuaag	miR-302a	uaagugcuuuccauguuuugguga
miR-145	guccaguuuuucccaggaaucuuu	miR-30a-3p	cuuucagucggauuuugcagc
miR-146	ugagaacugaaauuccauggguu	miR-30b	uguaaacaucuccacacucagc
miR-148a	ucagugcucuacagaaucuuu	miR-30c	uguaaacaucuccacacucagc
miR-149	ucuggcucggugucuuacucc	miR-30d	uguaaacaucucccagucggaag
miR-150	ucucccaacccuuguaaccagug	miR-30e	uguaaacaucuccuagucgga
miR-152	ucagugcagacagaaucuuug	miR-320	aaaagcugggguagagggcgaa
miR-154	uagguuuuacgguguuugcuucg	miR-323	gcacuuuacaggcugacucucu
miR-15a	uagcagcacauaauuguuuug	miR-324-5p	cgcaucccuuagggcgaugugugu
miR-15b	uagcagcacauaauuguuuua	miR-328	cuggccuccucugcccuuuccgu
miR-16	uagcagcacgaaauuauugcg	miR-331	gccccuggggccuauccuagaa
miR-17-5p	caaagugcuuacagugcagguagu	miR-335	ucaagagacaaauacgaaauuugu
miR-181a	aacauucaacgcugucggugagu	miR-338	uccagcaucaguguuuuuugua
miR-181b	aacauucaacgcugucggugguu	miR-339	ucccuguccucaggagcuca
miR-181c	aacauucaacgcugucggugagu	miR-340	uccgucucaguuuauuuuagcc
miR-182	uuugcgaauuguaaacucaca	miR-342	ucucacacagaaucgcacccguc
miR-183	uauggcacugguagaauuacug	miR-9	uccuuugguuuacugcuuagua
miR-184	uggagcggaagaacuguaaagggu	miR-9*	uaaagcuagaaacccaagaag
miR-185	uggagagaagagcgaucuc	miR-98	ugaggguaguuuuguuuuguu
miR-186	caaagaaauucuccuuuugggcu		

assay controls were included to verify optimal PCR efficiency. Previous studies using this kit have shown that microRNAs can be efficiently and reliably be detected over a large dynamic range up to a cycle threshold (Ct) value of 39 [17]. Only microRNAs that showed a Ct value of 40 were therefore considered not detectable. Relative expression numbers were calculated by the $\Delta\Delta C_t$ method in which the Ct of a specific microRNA is subtracted from the average Ct of two widely used housekeeping microRNAs, let-7a and miR-16 [19,20], and raising two to the power of this difference. The average expression level of the two housekeeping genes was thus arbitrarily set as 1 for normalization purposes. The average Ct of two housekeeping microRNAs was used to exclude the possibility that changes in the relative expression were caused by variations in the expression of the separate housekeeping microRNAs. Respective average housekeeping Ct values were 23.0±0.5 (let-7a) and 23.0±0.1 (miR-16) for chow-fed mice and 23.3±0.5 (let-7a) and 22.9±0.1 (miR-16) for WTD-fed mice.

2.5. Microarray gene expression analysis

The Mouse Genome Survey Arrays used in the study contained 33,012 different probes representing 26,514 genes, which included transcripts from the public

Table 2
Plasma lipids in LDLR^{-/-} mice fed a regular chow (CHOW) or WTD for 2 weeks

	CHOW	WTD	P
Total cholesterol	241±15	1600±98	<.001
VLDL cholesterol	9±1	585±64	<.001
LDL cholesterol	126±9	777±43	<.001
HDL cholesterol	92±9	195±5	<.001
Triglycerides	73±5	555±48	<.001

domain as well as from the Celera library. Total RNA from hepatocytes from LDLR^{-/-} mice fed a regular chow diet or WTD for 2, 4 or 6 weeks *ad libitum* was as described above. Double stranded cDNA was prepared from 2 µg of total RNA. An *in vitro* transcription reaction was used to synthesize 50–100 µg of UTP-digoxigenin-labeled complementary RNA (cRNA). Equal amounts of cRNA (10 µg) from two pooled RNA samples of two mice (total of four mice) per time point was hybridized to Mouse Genome Survey Arrays for 16 h at 55°C. Subsequently, an alkaline phosphatase-linked digoxigenin antibody was incubated with the array, and the phosphatase activity was initiated to start the chemiluminescent signal. The chemiluminescent (cRNA) and fluorescent (spot background) signals of the cRNA and standard controls spots were scanned for 5 and 25 s using an AB1700 Chemiluminescence Analyzer (Applied Biosystems). Using the software supplied with the AB1700 apparatus, the spot chemiluminescent signal was normalized over the fluorescent signal of the same spot (using the standard control signals) to obtain the normalized signal value that was used for further analysis. In the analysis, the median value of the normalized signal of two independent arrays for each time point was calculated as an indication for the relative gene expression number at that time point.

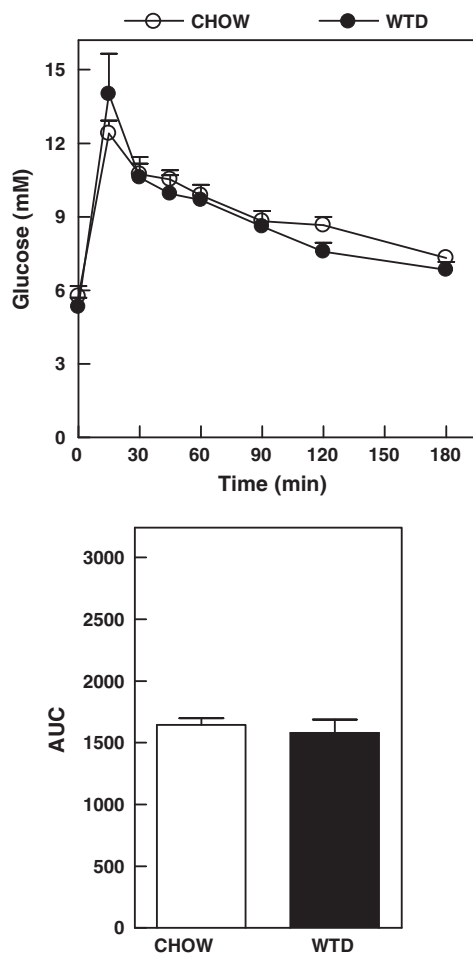


Fig. 1. Blood glucose kinetics during an OGTT. An OGTT was performed in overnight fasted LDLR^{-/-} mice that were fed a regular chow diet (CHOW; open circles and white bars) and those fed a WTD (filled circles and black bars) for 2 weeks. The blood glucose levels in time (top) and the AUC (bottom) was calculated. Data represent means±S.E.M.

2.6. Statistical analyses

Statistical differences in the relative microRNA expression profiles were determined with two-way ANOVA with Bonferroni posttest and corrected for multiple testing if appropriate using GraphPad InStat software (www.graphpad.com). *P* values <.05 were considered significant. Data are presented as means±S.E.M.

3. Results

To identify microRNA targets possibly involved in the development of fatty liver/hepatic steatosis, we have profiled the expression levels of 103 murine microRNAs in hepatocytes isolated from LDLR^{-/-} mice that were fed a high-fat WTD containing 0.25% cholesterol and 15% fat for 2 weeks *ad libitum*. Under Western-type feeding conditions, LDL receptor knockout mice exhibit severe hyperlipidemia, *i.e.*, hypertriglyceridemia and a marked 6- to 63-fold increase in the levels of apolipoprotein B-containing lipoproteins very low-density and low-density lipoproteins (VLDL and LDL, respectively) in plasma (Table 2). Previous studies have shown that this rapid rise in plasma lipids in LDL receptor knockout mice upon WTD feeding is associated with hepatic steatosis, *i.e.*, the accumulation of both cholesterol and triglycerides in hepatocytes [15] and insulin and glucose tolerance [16]. In accordance, we could macroscopically observe a clear fat-induced whitening of the livers in mice that were subjected to WTD

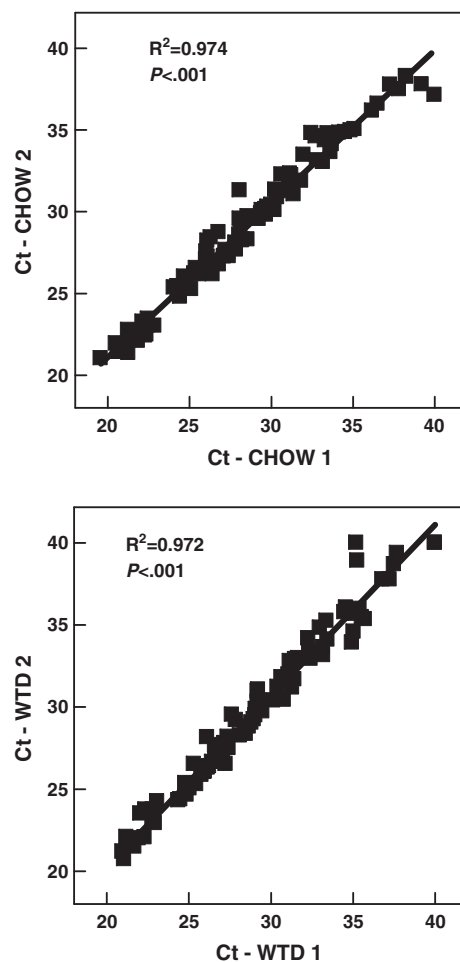


Fig. 2. Correlations of the microRNA expression (given as Ct numbers) between the different pools of RNA isolated from hepatocytes of LDLR^{-/-} mice on a regular chow (CHOW) diet or a WTD for 2 weeks. Only detectable microRNAs (Ct<40) were included in the analysis. A highly significant correlation ($R^2 > .97$) is observed in Ct values between the different pools of RNA.

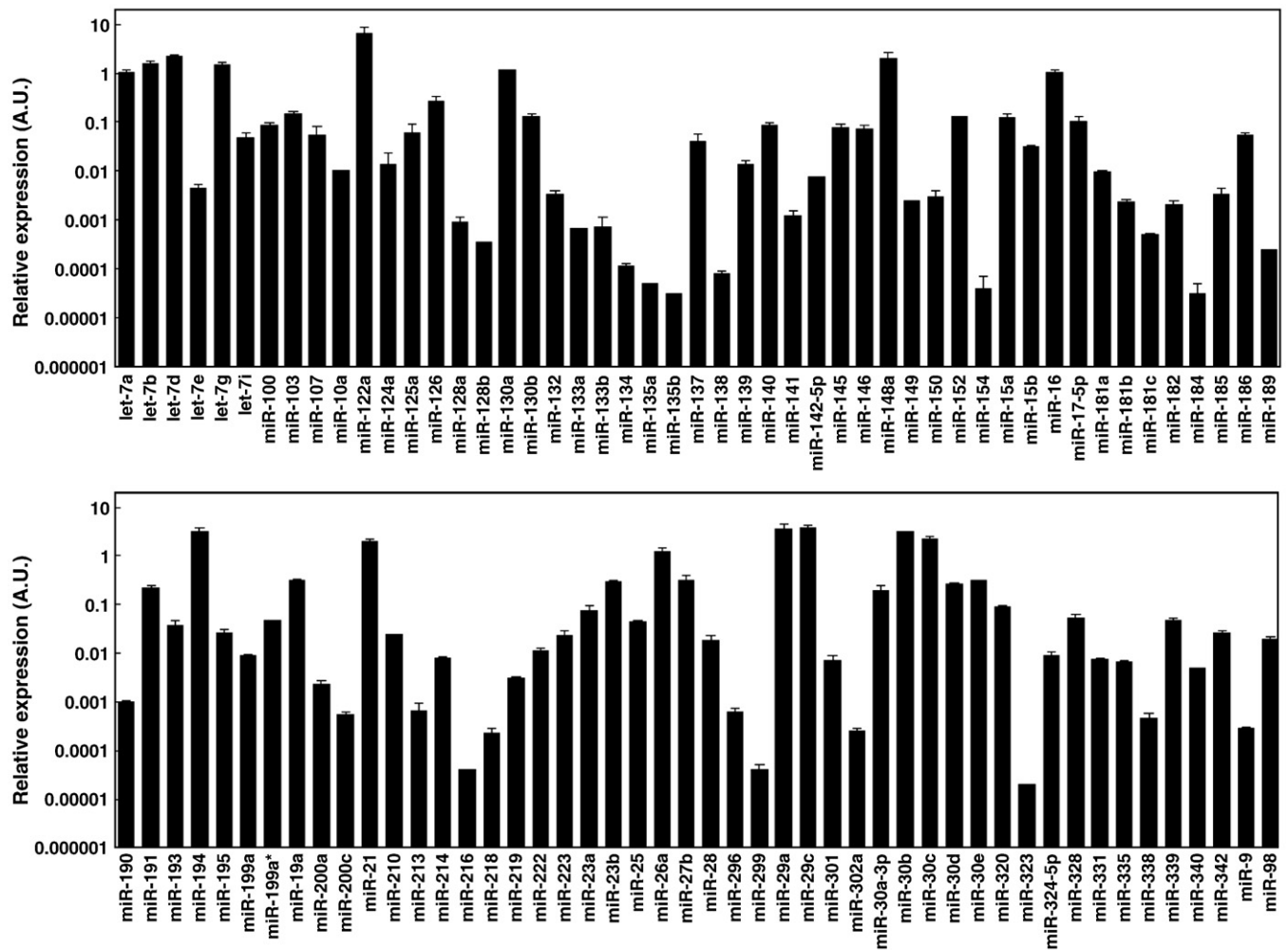


Fig. 3. Relative expression levels of the 97 microRNAs detected in hepatocytes from LDLR^{-/-} mice on a regular chow diet. Data are expressed relative to average expression level of the housekeeping microRNAs let-7a and miR-16 and represent means \pm S.E.M.

feeding (data not shown). However, in the current study, feeding the WTD for only 2 weeks did not yet affect the glucose tolerance (Fig. 1).

Of the total 103 microRNAs measured, 97 microRNAs were actually expressed by hepatocytes from mice fed either chow or WTD for 2 weeks. Four microRNAs were identified as not being expressed ($Ct \geq 40$ in all samples), including miR-9*, miR-125b, miR-127 and miR-205. Of note, individual microRNA expression levels significantly correlated across the various hepatocyte pools ($R^2 = .974$ and $P < .001$ for chow; $R^2 = .972$ and $P < .001$ for WTD; Fig. 2), suggestive of a low variability of hepatic microRNA expression levels between mice. As evident from Fig. 3, the relative expression level of the different microRNAs varied greatly in hepatocytes of mice fed the control (low-fat) chow diet. miR-122a was identified as being the most highly expressed microRNA (relative expression vs. housekeeping = 6.5), which is in agreement with previous findings in total liver specimens [21]. Two-way ANOVA with correction for multiple testing on the microRNA expression profiles indicated that the microRNA signature was essentially the same between hepatocytes isolated from mice fed chow or WTD. More specifically, the separate microRNAs, the type of diet and the interaction between the two variables contributed for 98.7% ($P < .001$), 0.00% ($P = .67$) and 0.54% ($P = .038$), respectively, to the total variation in the microRNA signature. The ANOVA Bonferroni posttest, however, revealed that the expression of two specific microRNAs was different between chow- and WTD-fed mice. A significant fivefold decrease in the

relative expression level of both miR-216 ($P < .05$) and miR-302a ($P < .01$) was detected in hepatocytes under the high lipid conditions (Fig. 4). Importantly, the lowering effect of the WTD on the expression of both miR-216 and miR-302a could be verified in an independent

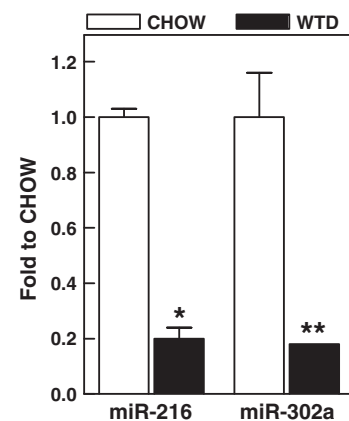


Fig. 4. The relative expression level of the microRNAs miR-216 and miR-302a that were differentially expressed between hepatocytes from LDLR^{-/-} mice fed a regular chow diet (CHOW; white bars) and those fed a WTD (black bars) for 2 weeks. Data represent means \pm S.E.M. * $P < .05$, ** $P < .01$ (two-way ANOVA).

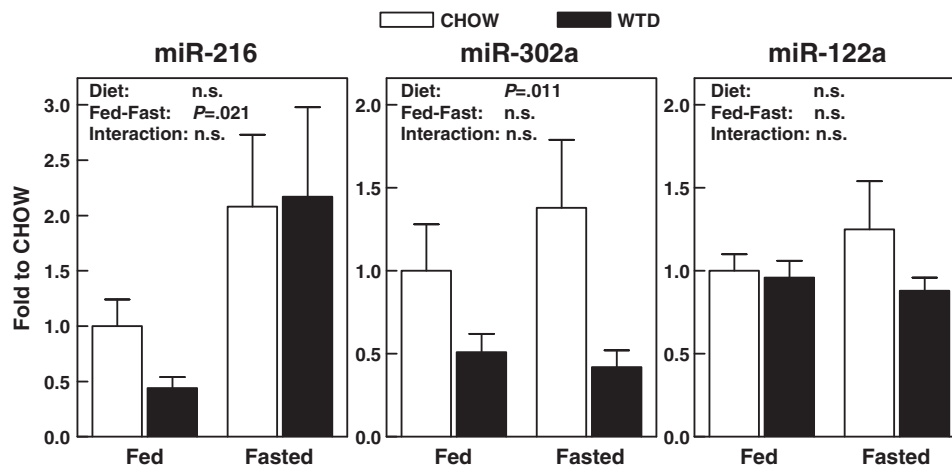


Fig. 5. The relative expression level of specified microRNAs in livers from LDLR^{-/-} mice fed a regular chow diet (CHOW; white bars) or a WTD (black bars) for 2 weeks and that were subjected to overnight fasting (Fasted) or fed *ad libitum* (Fed) before sacrifice. Data represent means \pm S.E.M. Statistical significances (*P* values) indicated in the different panels are derived from two-way ANOVA.

experiment using whole liver specimens from LDLR^{-/-} mice. In the *ad libitum* fed state, the relative expression level of miR-216 and miR-302a was respectively 56% and 49% decreased in livers from mice fed the WTD as compared with that on chow diet (Fig. 5). Tovar *et al.* [22] have previously detected an inverse correlation between insulin-like growth factor (IGF) activation and miR-216 levels in hepatocellular carcinoma. Importantly, in line with diminished (hepatic) insulin signaling in the fasting state, miR-216 expression in livers of mice fed the regular chow diet markedly increased upon fasting of mice (108% vs. fed state). Furthermore, fasting abolished the WTD-induced decrease in the hepatic expression level of miR-216 as observed in the *ad libitum* fed state ($P < .05$ for fasting effect; Fig. 5), resulting in an equally high level of miR-216 in fasted mice of either diet group. This suggests that metabolic factors other than the dietary lipid content, *i.e.*, plasma insulin/IGF levels, also to a great extent influence the hepatocyte relative expression level of miR-216. In contrast, a similar WTD-induced decrease in the expression of miR-302a was observed in livers from mice that were or were not subjected to overnight fasting before sacrifice, further establishing the importance of the high intrahepatic lipid pressure in the regulation of hepatocyte miR-302a expression ($P < .05$ for diet effect; Fig. 5). In accordance with the general view that highly expressed microRNAs are “housekeeping microRNAs,” no change, however, was observed in miR-122a expression upon WTD feeding or in response to fasting in whole liver specimens (Fig. 5).

To determine whether miR-216 and miR-302a are directly involved in the control of hepatic lipid metabolism, a microRNA/target gene/biological function linkage analysis was performed *in silico* using the PicTar algorithm for the prediction of microRNA targets (<http://pictar.mdc-berlin.de>). For miR-216, we extracted 67 target genes, while 224 target genes were indicated to be responsive to the miR-302a. We subsequently categorized putative target genes by the PANTHER classification system (<http://www.pantherdb.org>), which is a database that classifies genes into families and subfamilies of shared function and identified pathways that are enriched in the list of microRNA targets. Transcripts associated with biological processes involved in basic cell cycle control and cell proliferation and differentiation such as nucleoside, nucleotide and nucleic acid metabolism and nuclear transport were greatly overrepresented (more than twofold) with a high probability ($P < .01$) in the list of miR-216 and miR-302a targets (Table 3), which concurs with recent findings of Card *et al.* [23] and Kushibiki [24] that suggest a role for these two miRNAs in the induction of cell cycle arrest and apoptosis. In contrast, biological processes associated with lipid metabolism

were not significantly overrepresented in the total list of miR-216/miR-302a targets. However, the miR-216/miR-302a target list does contain genes associated with pathways involved in cholesterol, (phospho)lipid, fatty acid and carbohydrate metabolism. For miR-216, these include HDL binding protein (HDLBP; vigilin), phosphatase and tensin homolog (PTEN) and adiponectin receptor 1 (ADIPOR1), while myotubularin-related protein 4 (MTMR4), phosphatidylinositol-4-phosphate 5-kinase type II alpha (PIP5K2A), ATP-binding

Table 3

Biological pathways that were significantly overrepresented in the list of predicted mouse miR-216/302a target genes ($P < .05$; PANTHER software)

Pathway	No. observed in miR-216/302a targets	No. expected from public database	<i>P</i>
Nucleobase, nucleoside, nucleotide and nucleic acid metabolic process	106	45	9.63E−19
Primary metabolic process	167	98	6.41E−17
Metabolic process	168	103	5.25E−15
Cell cycle	51	22	1.15E−08
Developmental process	67	36	1.94E−07
System development	50	24	5.68E−07
Nervous system development	34	15	7.05E−06
Cellular process	110	77	1.20E−05
Mesoderm development	37	18	4.16E−05
Intracellular signaling cascade	37	19	5.24E−05
Ectoderm development	34	17	7.35E−05
Signal transduction	78	52	1.18E−04
Cell communication	79	54	2.22E−04
Mitosis	18	7	3.63E−04
Nuclear transport	6	1	5.46E−04
Muscle organ development	15	6	8.33E−04
Embryonic development	15	6	9.82E−04
Segment specification	9	3	1.72E−03
Skeletal system development	14	6	1.92E−03
Apoptosis	22	11	2.12E−03
Response to stress	14	6	2.77E−03
Pattern specification process	11	4	4.88E−03
Protein metabolic process	59	43	6.18E−03
Gamete generation	20	11	6.92E−03
Negative regulation of apoptosis	8	3	1.59E−02
Cell surface receptor linked signal transduction	41	29	1.60E−02
Reproduction	20	12	1.76E−02
Cellular component organization	26	17	2.21E−02
Induction of apoptosis	9	4	2.44E−02
Coenzyme metabolic process	4	1	3.12E−02
Female gamete generation	7	3	4.75E−02

cassette transporter A1 (ABCA1), long-chain fatty acid elongation 6 (ELOVL6), alkylglycerone phosphate synthase (AGPS), receptor accessory protein 3 (REEP3) and forkhead box J3 (FOXJ3) are putative lipid-associated targets of miR-302a. Previously, we have performed large scale microarray gene expression profiling to identify specific pathways and genes involved in the response of hepatocytes from LDLR^{-/-} mice to increased dietary lipid levels [25]. To determine whether the inhibition of miR-216 and miR-302a expression in hepatocytes on WTD was paralleled by a decrease in their regulatory activity, we extracted from our original microarray dataset the time-dependent expression profiles of their respective target genes. Gene expression of *HDLBP*, *PTEN*, *ADIPOR1*, *ABCA1*, *ELOVL6*, and *REEP3* was detected in hepatocytes of LDLR^{-/-} mice fed a WTD for 0, 2, 4 and 6 weeks, while *MTMR4*, *FOXJ3*, *AGPS* and *PIP5K2A* were identified as not being expressed in hepatocytes. As depicted in Fig. 6, no major changes (more than two fold change) in the relative expression levels of the miR-216 targets *HDLBP*, *PTEN* and *ADIPOR1* and the miR-302a target *REEP3* were observed upon WTD feeding. In contrast, in accordance with a diminished miR-302a expression/function, the relative expression levels of the miR-302a targets *ABCA1* and in particular *ELOVL6* were increased in response to the WTD (twofold to ninefold; Fig. 6) in hepatocytes of LDLR^{-/-} mice.

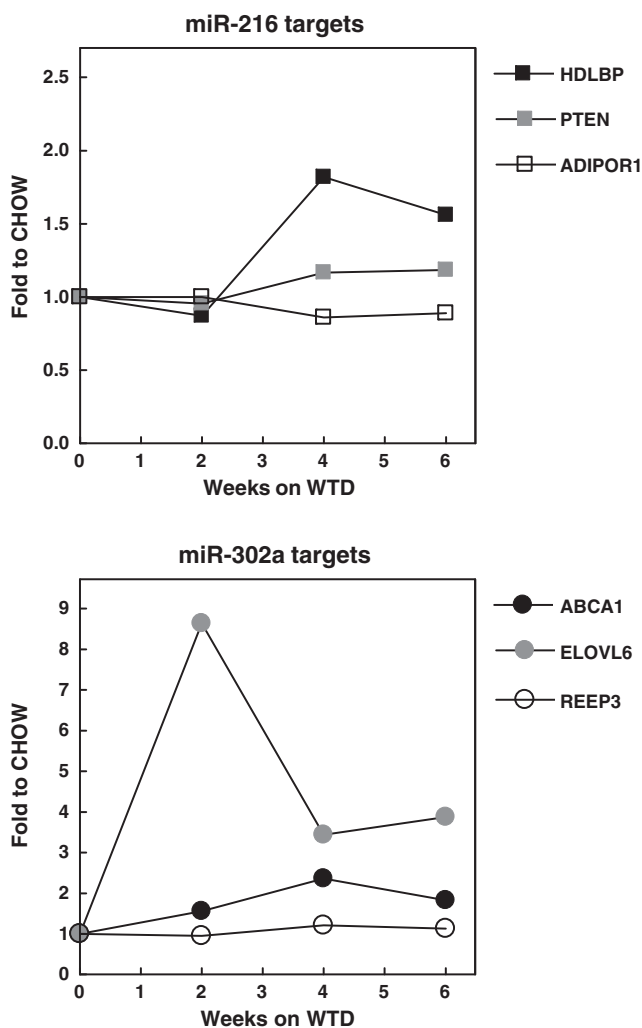


Fig. 6. Relative mRNA expression levels of miR-216 and miR-302a target genes that are associated with lipid metabolism in hepatocytes from LDLR^{-/-} mice fed a WTD for 2, 4 or 6 weeks, as determined by microarray analysis. Data are presented as fold compared with relative expression values on chow diet.

4. Discussion

In the current study we profiled murine hepatocyte microRNA levels during nonalcoholic fatty liver development. Our data suggest an important role for miR-216 and miR-302a in the control of hepatic metabolism upon a high lipid stimulus as the relative expression level of these two microRNAs is significantly decreased in response to WTD feeding. However, from our microarray gene expression analysis in hepatocytes under the dietary conditions, it seems that the decrease in miR-216 expression is not associated with a parallel increase in the expression of miR-216 target genes involved in hepatic metabolism. This argues against a major role for miR-216 in the control of hepatic lipid homeostasis. In contrast, the decrease in miR-302a expression in hepatocytes coincided with a marked ninefold increase in the expression of the miR-302a target gene *ELOVL6*. *ELOVL6* belongs to a highly conserved family of microsomal enzymes involved in the formation of long-chain fatty acids [26]. *ELOVL6* has a role in the elongation of palmitate (16:0) to stearate (18:0), as well as in the elongation of palmitoleate (16:1n-7) to vaccinate (18:1n-7) [27]. Importantly, although *ELOVL6*-deficient mice become obese and do develop hepatic steatosis to a similar extent as their wild-type littermate controls when fed a high-fat diet, they are protected from hyperinsulinemia, hyperglycemia and hyperleptinemia [26]. Combined, these findings suggest that the decrease in hepatic miR-302a activity, which coincides with an up-regulation of *ELOVL6* gene expression, is not the initial cause for the development NAFLD but may rather predispose the liver to the (hepatic) insulin resistance that occurs at later stages of the disease. Hepatic insulin resistance is one of the major characteristics of the metabolic syndrome, a prominent risk factor for the development of cardiovascular disease [28]. Further studies will be needed to prove the importance of miR-302a in the regulation of hepatic lipid metabolism and insulin resistance and reveal the potential of miR-302a as therapeutic target for the treatment of hepatic insulin resistance and associated cardiovascular diseases.

In conclusion, we have shown that WTD-induced nonalcoholic fatty liver development in LDL receptor knockout mice is associated with a significant change in the hepatocyte microRNA signature, i.e., a fivefold decrease in miR-216 and miR-302a expression. Based upon our comparative gene and microRNA expression studies, it is anticipated that miR-302a may prove to be a valuable therapeutic target in the regulation of hepatic fatty acid utilization and insulin resistance.

References

- [1] Jou J, Choi SS, Diehl AM. Mechanisms of disease progression in nonalcoholic fatty liver disease. *Semin Liver Dis* 2008;28:370–9.
- [2] Nelson P, Kiriakidou M, Sharma A, Maniatakis E, Mourelatos Z. The microRNA world: small is mighty. *Trends Biochem Sci* 2003;28:534–40.
- [3] Cheung O, Puri P, Eicken C, Contos MJ, Mirshahi F, Maher JW, et al. Nonalcoholic steatohepatitis is associated with altered hepatic microRNA expression. *Hepatology* 2008;48:1810–20.
- [4] Cheng AM, Byrom MW, Shelton J, Ford LP. Antisense inhibition of human miRNAs and indications for an involvement of miRNA in cell growth and apoptosis. *Nucleic Acids Res* 2005;33:1290–7.
- [5] Leaman D, Chen PY, Fak J, Yalcin A, Pearce M, Unnerstall U, et al. Antisense-mediated depletion reveals essential and specific functions of microRNAs in *Drosophila* development. *Cell* 2005;121:1097–108.
- [6] Esau C, Davis S, Murray SF, Yu XX, Pandey SK, Pear M, et al. miR-122 regulation of lipid metabolism revealed by in vivo antisense targeting. *Cell Metab* 2006;3:87–98.
- [7] Krützfeldt J, Rajewsky N, Braich R, Rajeev KG, Tuschl T, Manoharan M, et al. Silencing of microRNAs in vivo with 'antagomirs'. *Nature* 2005;438:685–9.
- [8] Li S, Chen X, Zhang H, Liang X, Xiang Y, Yu C, et al. Differential expression of microRNAs in mouse liver under aberrant energy metabolic status. *J Lipid Res* 2009;50:1756–65.
- [9] Hoekstra M, Kruijff JK, Van Eck M, Van Berkel TJ. Specific gene expression of ATP-binding cassette transporters and nuclear hormone receptors in rat liver parenchymal, endothelial, and Kupffer cells. *J Biol Chem* 2003;278:25448–53.

- [10] Hoekstra M, Out R, Kruijt JK, Van Eck M, Van Berkel TJ. Diet induced regulation of genes involved in cholesterol metabolism in rat liver parenchymal and Kupffer cells. *J Hepatol* 2005;42:400–7.
- [11] Ye D, Hoekstra M, Out R, Meurs I, Kruijt JK, Hildebrand RB, et al. Hepatic cell-specific ATP-binding cassette (ABC) transporter profiling identifies putative novel candidates for lipid homeostasis in mice. *Atherosclerosis* 2008;196:650–8.
- [12] Repa JJ, Lund EG, Horton JD, Leisersdorf E, Russell DW, Dietschy JM, et al. Disruption of the sterol 27-hydroxylase gene in mice results in hepatomegaly and hypertriglyceridemia. Reversal by cholic acid feeding. *J Biol Chem* 2000;275:39685–92.
- [13] Xie Y, Newberry EP, Kennedy SM, Luo J, Davidson NO. Increased susceptibility to diet-induced gallstones in liver fatty acid binding protein knockout mice. *J Lipid Res* 2009;50:977–87.
- [14] He S, McPhaul C, Li JZ, Garuti R, Kinch L, Grishin NV, et al. A sequence variation (I148M) in PNPLA3 associated with nonalcoholic fatty liver disease disrupts triglyceride hydrolysis. *J Biol Chem* 2010;285:6706–15.
- [15] Wouters K, van Gorp PJ, Bieghs V, Gijbels MJ, Duimel H, Lütjohann D, et al. Dietary cholesterol, rather than liver steatosis, leads to hepatic inflammation in hyperlipidemic mouse models of nonalcoholic steatohepatitis. *Hepatology* 2008;48:474–86.
- [16] Mulvihill EE, Allister EM, Sutherland BG, Telford DE, Sawyez CG, Edwards JY, et al. Naringenin prevents dyslipidemia, apolipoprotein B overproduction, and hyperinsulinemia in LDL receptor-null mice with diet-induced insulin resistance. *Diabetes* 2009;58:2198–210.
- [17] Chen C, Ridzon DA, Broomer AJ, Zhou Z, Lee DH, Nguyen JT, et al. Real-time quantification of microRNAs by stem-loop RT-PCR. *Nucleic Acids Res* 2005;33:e179.
- [18] Chomczynski P, Sacchi N. Single-step method of RNA isolation by acid guanidinium thiocyanate–phenol–chloroform extraction. *Anal Biochem* 1987;162:156–9.
- [19] Slaby O, Svoboda M, Fabian P, Smerdova T, Knoflickova D, Bednarikova M, et al. Altered expression of miR-21, miR-31, miR-143 and miR-145 is related to clinicopathologic features of colorectal cancer. *Oncology* 2007;72:397–402.
- [20] Wong TS, Liu XB, Wong BY, Ng RW, Yuen AP, Wei WI. Mature miR-184 as potential oncogenic microRNA of squamous cell carcinoma of tongue. *Clin Cancer Res* 2008;14:2588–92.
- [21] Chang J, Nicolas E, Marks D, Sander C, Lerro A, Buendia MA, et al. miR-122, a mammalian liver-specific microRNA, is processed from hcr mRNA and may downregulate the high affinity cationic amino acid transporter CAT-1. *RNA Biol* 2004;1:106–13.
- [22] Tovar V, Alsinet C, Villanueva A, Hoshida Y, Chiang DY, Solé M, et al. IGF activation in a molecular subclass of hepatocellular carcinoma and pre-clinical efficacy of IGF-1R blockade. *J Hepatol* 2010;52:550–9.
- [23] Card DA, Hebbbar PB, Li L, Trotter KW, Komatsu Y, Mishina Y, et al. Oct4/Sox2-regulated miR-302 targets cyclin D1 in human embryonic stem cells. *Mol Cell Biol* 2008;28:6426–38.
- [24] Kushibiki T. Photodynamic therapy induces microRNA-210 and -296 expression in HeLa cells. *J Biophotonics* 2010;3(5–6):368–72.
- [25] Hoekstra M, Stitzinger M, van Wanrooij EJ, Michon IN, Kruijt JK, Kamphorst J, et al. Microarray analysis indicates an important role for FABP5 and putative novel FABPs on a Western-type diet. *J Lipid Res* 2006;47:2198–207.
- [26] Leonard AE, Pereira SL, Sprecher H, Huang YS. Elongation of long-chain fatty acids. *Prog Lipid Res* 2004;43:36–54.
- [27] Matsuzaka T, Shimano H, Yahagi N, Kato T, Atsumi A, Yamamoto T, et al. Crucial role of a long-chain fatty acid elongase, Elovl6, in obesity-induced insulin resistance. *Nat Med* 2007;13:1193–202.
- [28] Andreassi MG. Metabolic syndrome, diabetes and atherosclerosis: influence of gene–environment interaction. *Mutat Res* 2009;667:35–43.